

# Dissolution profiles of partially purified bromelain from pineapple cores [*Ananas comosus* (L.) Merr] encapsulated in glutaraldehyde-crosslinked chitosan

Siswati Setiasih\*, Hegi Adi Prabowo, Emil Budianto, Sumi Hudiyono

Department of Chemistry, Faculty of Mathematics and Natural Sciences, Universitas Indonesia, Depok, Indonesia.

## ARTICLE INFO

Received on: 16/08/2018

Accepted on: 11/10/2018

Available online: 31/10/2018

### Key words:

Bromelain, purification, post-loading encapsulation, crosslinked chitosan, dissolution.

## ABSTRACT

To avoid degradation in the stomach, the proteolytic enzyme bromelain must be encapsulated in glutaraldehyde-crosslinked chitosan (CGF) hydrogels, which can maintain the activity of bromelain until it reaches the intestine. In this study, we isolated bromelain by using ammonium sulfate precipitation, dialysis, and anionic exchange chromatography with Diethylaminoethyl (DEAE)-cellulose resin. Bromelain fractions were collected from each purification step and specific activities were sequentially from increased in the crude enzyme, ammonium sulfate, dialysis, and DEAE chromatography fractions (fraction numbers 58–71), which have fractions of 23.90, 122.00, 125.48, and 195.20 U/mg, respectively. Bromelain fractions from the dialysis step were encapsulated in CGF matrixes by using a post-loading method. CGF hydrogels had a crosslinking degree of 84.37% and swelling ratio of 76.60%. The dissolution profiles of CGF-encapsulated bromelain were tested in artificial stomach fluid and intestinal environments, and bromelain encapsulation efficiency following the post-loading method was 96.29%. Interactions between the hydrogel and bromelain were limited to the hydrogen bonds, and the proteolytic activities of bromelain were maintained at 0.17 U/ml in the present artificial intestinal environment.

## INTRODUCTION

The per capita pineapple consumption of Indonesia increased by an average of 1.93% per year during 2002–2014, and 1.73 tons of pineapple was produced in 2015 (Respati, 2016). This increase in pineapple consumption was accompanied by the increased availability of pineapple waste products, including stems, skins, and cores. These wastes contain proteases that could be exploited in other applications (Ketnawa *et al.*, 2012). The protease bromelain has a wide range of therapeutic effects, such as an antitumor agent, a platelet aggregation inhibitor, and an antibiotic absorption enhancer (Costa *et al.*, 2014). Oral treatments with bromelain are complicated by contact with stomach fluids, which degrade the enzyme. In a previous study,

the proteolytic activities of bromelain were decreased in artificial stomach fluids but were relatively stable over the first 4 hours (Setiasih *et al.*, 2018). Decreases in bromelain proteolytic activity followed deactivation and degradation by acidic stomach fluids and stomach enzymes. After encapsulation into controlled drug delivery devices, bromelain was absorbed into human intestines without losing activity (Chobotova *et al.*, 2010). Hydrogels are widely used as raw materials for encapsulation and can swell owing to their hydrophilic and porous properties; therefore, these materials provide ease of design and control of crosslinking densities in matrixes (Gonçalves *et al.*, 2005; Zhao *et al.*, 2002). Chitosan-based hydrogels are widely used in many fields due to its excellent biodegradability, economic efficiency, and biocompatibility. These properties show that crosslinked-chitosan matrixes can be used as coating materials for controlled drug delivery systems. Furthermore, crosslinked-chitosan has a lot of primary amino groups ( $-NH_2$ ) which can bind to biomolecules such as protein and DNA easily (Ou and Bo, 2017). In the present study, we crosslinked-chitosan by using glutaraldehyde

\*Corresponding Author

Siswati Setiasih, Department of Chemistry, Faculty of Mathematics and Natural Sciences, Universitas Indonesia, Depok, Indonesia.

E-mail: [setiasih@ui.ac.id](mailto:setiasih@ui.ac.id)

and used the resulting preparation to coat bromelain from pineapple cores by using a post-loading method. Controlled drug delivery using this system was then evaluated in artificial stomach fluid (pH 1.2) and intestinal environments (pH 7.4) (Yadav and Shivakumar, 2012).

## MATERIALS AND METHODS

### Materials

Chitosan was purchased from CV. Bio Chitosan Indonesia. All other chemical reagents were purchased from Sigma-Aldrich.

### Isolation and ammonium sulfate fractionation of bromelain

Pineapple cores were cut into pieces and crushed by using a blender under cold conditions. Core solutions were then filtered by muslin, and filtrates were centrifuged at 6,000 rpm for 40 minutes at  $\pm 4^{\circ}\text{C}$ . The resulting supernatants were designated crude enzyme fractions and were further fractionated for 20 minutes under cold conditions by using ammonium sulfate at concentrations of 0%–20%, 20%–50%, and 50%–80% of the crude enzyme volume. Fractions were stored overnight ( $\pm 12$  hours) at  $4^{\circ}\text{C}$  and were then centrifuged at 6,000 rpm for 15 minutes at  $4^{\circ}\text{C}$ . Precipitates were finally suspended in cold solutions of 0.2 M phosphate buffer at pH 7 (Devakate *et al.*, 2009).

### Dialysis

Dialysis membranes containing enzymes were soaked in 100 ml of 0.05 M phosphate buffer at pH 7.0 with continuous stirring at  $4^{\circ}\text{C}$ . Every 2 hours, phosphate buffer was replaced with fresh buffer phosphate, and precipitates were formed using 5% (w/v)  $\text{BaCl}_2$  in acidic solution. The absence of  $\text{BaSO}_4$  precipitates indicated that dialysis was complete (Gautam *et al.*, 2010).

### Purification by anion exchange chromatography

Dialyzed enzymes were purified using anion exchange chromatography with a combination of stepwise and gradient elution. Enzyme solutions containing enzymes at up to 5% (v/v) were added to columns containing DEAE-cellulose resin as the stationary phase. Columns were then eluted using 0.05 M Tris-HCl buffer (pH 8) and then Tris-HCl containing NaCl at 0.25, 0.50, 0.70, and 1.00 M with a flow rate of 1.5 ml/minute (Gautam *et al.*, 2010). Eluents were collected in fraction vials (5 ml/tube), and the absorbance of fractions was determined using UV-Vis spectrophotometry at 280 nm. Data were graphed by plotting absorbance values against fraction numbers, and protein peaks were then calculated. The proteolytic activities of each fraction were finally analyzed and fractions were grouped to determine specific activity (Setiasih *et al.*, 2018).

### Determinations of proteolytic activities and protein contents

The proteolytic activities of the enzyme were determined according to the Kunitz method with some modifications by using a UV-Vis spectrophotometer at 280 nm. The total protein contents of fractions were determined using the Lowry method according to the absorbance at 595 nm (Musfiroh *et al.*, 2018).

### Synthesis of chitosan film and CGF

Chitosan hydrogel was synthesized by adding 2 g of chitosan to 98 ml of 1% (v/v) acetic acid and then stirring at room temperature until the mixture became homogeneous. Noncovalent Chitosan Film (CF) was produced by molding the chitosan solution into a film and drying in an oven at  $60^{\circ}\text{C}$  overnight. CGF was synthesized by adding 0.1 M glutaraldehyde at 10% (v/v) to 2% chitosan solution and then stirring for 2 hours. The mixture was then molded into a film and was dried at  $60^{\circ}\text{C}$  for 12 hours. Hydrogels were stored in a desiccator before further use. CF and CGF were analyzed using Fourier transform infrared spectroscopy (FTIR) and optical microscopy (Budianto *et al.*, 2015).

### Determination of degrees of crosslinking

Dry CF and CGF films were weighed and soaked in 1% acetic acid for 24 hours. CF and CGF were then removed and dried in an oven at  $60^{\circ}\text{C}$ , and dry weights were recorded from before and after soaking. The degrees of crosslinking were calculated using the following equation (Abdel-Mohzen *et al.*, 2011):

$$\% \text{ Degree of crosslinking} = \frac{W_g}{W_0} \times 100\%,$$

where  $W_g$  is the initial weight of the dry film and  $W_0$  is the weight of the dry film after soaking in acetic acid.

### Determination of swelling ratios

CF and CGF were weighed and soaked in phosphate buffer (pH 7.0) for 30 minutes at room temperature, and the remaining water on the surface of the hydrogel was removed. The wet weights of CF and CGF were then determined, and the swelling ratios were calculated using the following equation (Selvakumaran *et al.*, 2016):

$$\text{Swelling ratio (\%)} = \frac{W_{\text{wet}} - W_{\text{dry}}}{W_{\text{dry}}} \times 100\%.$$

### Encapsulation of bromelain using the post-loading method

Bromelain enzyme dialysis fractions of 0.1 ml were dropped into dry CFG, and the enzyme was then stored overnight to complete the encapsulation process. CFG surfaces containing bromelain were rinsed using 0.2 M phosphate buffer (pH 7). The amounts and activities of loaded bromelain were then calculated using the following equation (Croisfelt *et al.*, 2015):

$$\text{Loaded bromelain} = [\text{Bromelain}]_{\text{initial}} - [\text{Bromelain}]_{\text{dishwater}}$$

$$\text{Loaded activity} = (U \text{ ml}^{-1})_{\text{initial}} - (U \text{ ml}^{-1})_{\text{dishwater}}.$$

Finally, CGF-encapsulated bromelain was analyzed using FTIR.

### In vitro dissolution testing

The dissolution profiles of bromelain in CGF were tested by placing CGF in 10 ml aliquots of HCl buffer (pH 1.2) and then incubating at  $37^{\circ}\text{C}$  with shaking at 100 rpm. After 2 hours, the proteolytic activity and total protein contents in artificial stomach fluids were determined. CGF from pH 1.2 buffer was finally

incubated at 37°C in phosphate buffer (pH 7.4) for 10 hours with shaking at 100 rpm, and the proteolytic activity and total protein contents in the artificial intestinal environment were then determined (Reddy *et al.*, 2018).

## RESULT AND DISCUSSION

### Isolation of crude enzyme

The Lowry method exploits the reduction of Cu(II)-protein bonds under alkaline conditions. Released Cu<sup>2+</sup> then oxidizes aromatic groups in amino acid side chains, thus resulting in the reduction of phosphomolybdotungstate to heteropolymolybdenum blue (Waterborg, 2002). The resulting color change is proportional to tyrosine and tryptophan contents and can be quantitated using UV-Vis absorbance. The determinations of proteolytic activity are optimal at 37°C (pH 7) for 30 minutes. The proteolytic activity of bromelain is proportional to the production of trichloroacetic acid-soluble L-tyrosine from casein substrate. The specific activities of core solution and crude enzyme are shown in Table 1. The specific activity of the crude enzyme was higher than that of the pineapple core solution, which lacks pineapple fibers.

### Fractionation with ammonium sulfate and dialysis

The fractionation of enzymes using ammonium sulfate is performed using the salting out principle, which is based on the stronger interactions between proteins than between proteins and solvents. High ammonium sulfate concentrations can dehydrate proteins in crude enzyme (dehydration process) preparations, thus causing aggregation and precipitation (Green and Hughes, 1955). Bromelain activities from fractionation and dialysis processes (Table 2) indicate increasing specific enzyme activities with processing steps. The highest specific activity was obtained from the second fraction, although high specific activity was also observed

after the first fractionation step, and the enzyme solutions from this step were refractionated using 0%–50% ammonium sulfate. Subsequently, bromelain had increasing specific activities and purity. Dialysis was performed using principles of diffusion, and dialysis decreased the proteolytic activity with increasing volumes of the more dilute enzyme. However, nonbromelain proteins also diffuse through dialysis membranes, thus resulting in the increased specific activity and purity of the remaining bromelain.

### Purification using anion exchange chromatography

Bromelain enzyme was purified using stepwise elution by an anion exchange chromatography column. In this process, proteins with relatively weaker binding are released and replaced by elution with low concentrations of NaCl, and proteins with stronger binding affinity are released in subsequent elution stages. By using anion exchange chromatograms from 4.47 ml elutes of bromelain dialysis (Fig. 1), four protein peaks were observed in plots of absorbance at 280 nm. The proteolytic activities of each fraction were then tested and five protein peaks were obtained. After elution with 0.75 M NaCl, a small protein peak was associated with the highest proteolytic activity. Fractions with the highest activity were then combined, and specific activities were determined (Table 3). The yield of combined fractions from anion exchange chromatography was small, thus reflecting the volume of enzyme added to the chromatography column. The highest specific activity of the enzyme was observed in the third protein peak (Pr3), which corresponded to the mixture of fractions 58–71 (AP3). As shown in Table 3, AP3 had the highest purity of bromelain, which was eluted with 0.75 M NaCl.

### CF and CGF

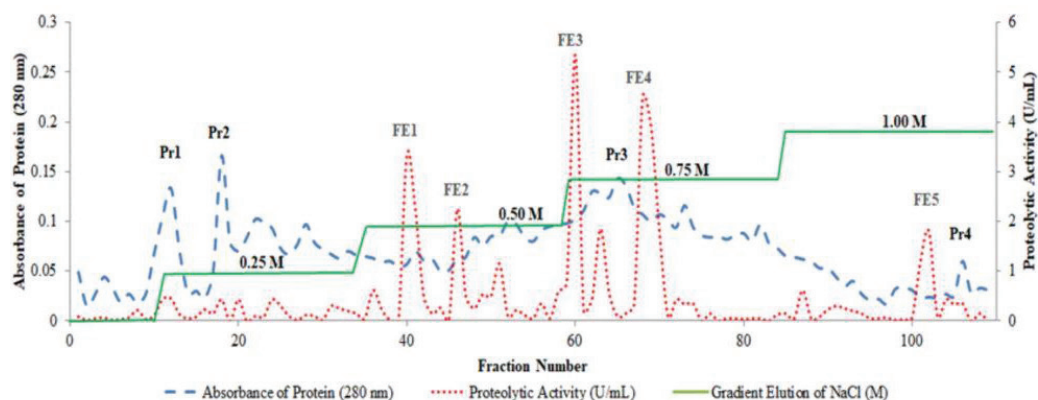
CGF was compared with CF to ensure that crosslinking reactions occurred. The compared parameters included morphology,

Table 1. Results of the bromelain isolation process.

Fraction	Volume (ml)	Total		Specific activity (U/mg)	Purification levels (fold)	%yield
		Protein content (mg)	Proteolytic activity (U)			
Homogenates were filtered, $T = \pm 4^{\circ}\text{C}$						
Core solution	250	71.16	937.50	13.18	-	-
Centrifuge 6,000 rpm, 45 minutes, $T = \pm 4^{\circ}\text{C}$						
Crude enzyme	103	27.65	660.92	23.90	1	100

Table 2. Bromelain activities after fractionation and dialysis.

Fraction	Volume (ml)	Total		Specific activity (U/mg)	Purification levels (fold)	%yield
		Protein content (mg)	Proteolytic activity (U)			
F1 (0%–20%)	6.6	1.24	81.62	66.06	2.77	12.35
F2 (20%–50%)	10	1.31	156.17	118.76	4.97	23.63
F3 (50%–80%)	2.2	0.27	9.53	35.27	1.48	1.44
F4 (remaining filtrate)	110	13.15	51.33	3.90	0.16	7.77
Re-fractionation						
F5 (0%–50%)	20	2.19	266.67	122.00	5.10	40.35
Dialysis						
F5 dialysis	22	2.04	256.30	125.48	5.25	38.78



**Figure 1.** Chromatogram from F5 dialysis (0%–50%) using a DEAE-cellulose matrix; Pr1–Pr4, the first to fourth protein peak at 280 nm; FE1–FE5, the first to fifth proteolytic activity peak; separation conditions: column diameter, 2.8 cm; column length, 50 cm; matrix volume, 89 cm<sup>3</sup>; elution flow rate, 1.5 ml/minutes; 5 ml fractions were collected, and elution was performed using a linear gradient and stepwise elution. The column was initially eluted with 0.05 M Tris-HCl buffer (pH 8.0) and then with the same buffer containing 0.25–1.0 M NaCl.

**Table 3.** Combined fraction from anion exchange chromatography using DEAE-cellulose resin.

Fraction	Volume (ml)	Total		Specific activity (U/mg)	Purification levels (fold)	Yield (%)	Recovery (%)
		Protein content (mg)	Proteolytic activity (U)				
AP1 (11–23)	65	0.14	5.42	38.58	1.61	0.82	33.33
AP2 (40–52)	65	0.04	3.25	86.21	3.61	0.49	9.52
AP3 (58–71)	70	0.08	15.17	195.20	8.17	2.30	19.05
AP4 (100–106)	35	0.02	0.58	28.74	1.20	0.09	4.76

FTIR spectra, swelling ratios, and crosslinking degrees. The morphological observations of CF and CGF were made using an optical microscope (Fig. 3a and b, respectively) and showed that the films were dense, smooth, and uniform. However, CF had greater volumes and was less rigid than CGF, thus reflecting the crosslinking reactions of chitosan and glutaraldehyde under acidic conditions. These conditions resulted in nucleophilic reactions that produced neutral carbinolamine. Subsequent acid catalysis protonated the hydroxyl groups of tetrahedral carbinolamine and eliminated water molecules to form iminium ions. Furthermore, H<sup>+</sup> ions that were bound with nitrogen were released, and neutral imine products with C=N bonds were formed. Such series of crosslinking reactions are known as Schiff base reactions (Banerjee *et al.*, 2010). The FTIR spectra of bromelain showed N–H stretch bands at 3,316 cm<sup>-1</sup>, C–H stretches at 2,929 cm<sup>-1</sup>, strong intensities of C=O stretch bands (amide 1 area) at 1,654 cm<sup>-1</sup>, and C–N stretch bands at 1,540 cm<sup>-1</sup> (Fig. 4a) (Bernela *et al.*, 2016). By contrast, chitosan spectra (Fig. 4b) showed a broadband at 3,500–3,080 cm<sup>-1</sup>, which resulted from the overlapping of O–H and N–H stretches. At a wave number of 1,659 cm<sup>-1</sup>, a C=O stretch band indicated the presence of amides from residual acetyl groups in chitosan. Moreover, an N–H bend stretch at 1,591 cm<sup>-1</sup> indicated the presence of primary amine groups. The saccharide structure (glycoside bridge) of C–O–C bands appeared at 1,037 cm<sup>-1</sup>. The dominant differences between CF and CGF were seen in the absorption band at a wave number of 1595 cm<sup>-1</sup>, with a C=N

stretch for imine groups of CGF that formed because of the Schiff base reactions between the carbonyl groups of glutaraldehyde and amine groups from chitosan (Fig. 4c and d) (Budianto *et al.*, 2015). The physical properties of CF and CGF were evaluated by determining the crosslinking degrees and swelling ratios. Hydrogels with high degrees of crosslinking were more rigid than hydrogels with low degrees of crosslinking. As shown in Table 4, the degrees of crosslinking for CGF were high compared with those of CF, thus suggesting that small parts of chitosan are soluble in acetic acid and that CGF has higher degrees of crosslinking than CF. The swelling ratios of hydrogels were investigated to determine the ability of hydrogels to absorb liquid (Table 4). The resulting data showed that the swelling ratios of CGF were lower than those of CF. In a previous study, hydrogel swelling was caused by repulsions between –NH<sub>3</sub><sup>+</sup> and amine groups in chitosan (Morris *et al.*, 2009). Given that the amine groups in CGF were subjected to crosslinking reactions with glutaraldehyde, fewer protonated amine groups were observed in CGF. The visual appearances of crosslinking and the swelling ratio tests of CGF are presented in Figure 2.

#### Encapsulation of bromelain in CGF

A post-loading encapsulation method was chosen to enhance the efficiency of encapsulation and to use fewer enzymes. The encapsulation efficiencies shown in Table 5 corresponded to the differing appearances of CGF before and



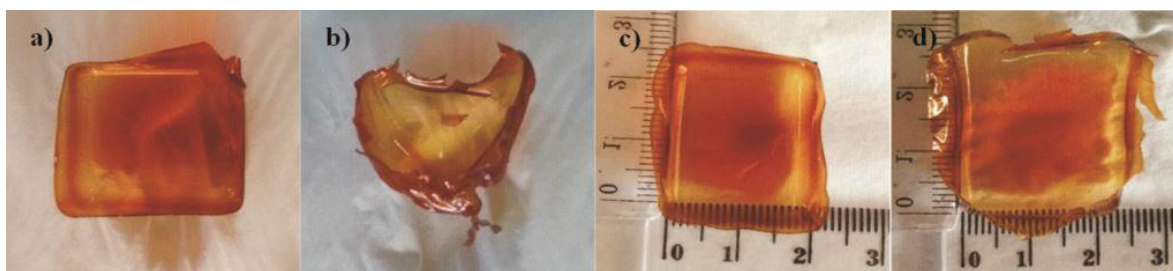


**Figure 2.** Visual appearances in tests of crosslinking degrees and swelling ratios of (a) CGF before testing the degrees of crosslinking, (b) CGF after testing the degrees of crosslinking, (c) CGF before the swelling ratio tests, and (d) CGF after the swelling ratio tests.

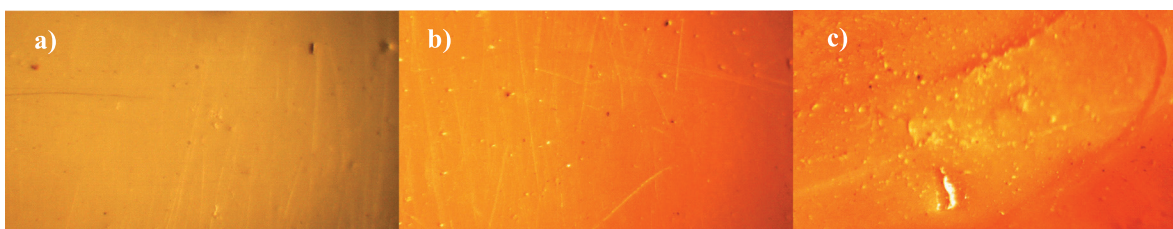


**Figure 3.** Morphological structure analyses using an optical microscope at 15 $\times$  magnification; (a) morphological structure of chitosan film; (b) morphological structure of CGF before encapsulation; and (c) morphological structure of CGF after encapsulation.

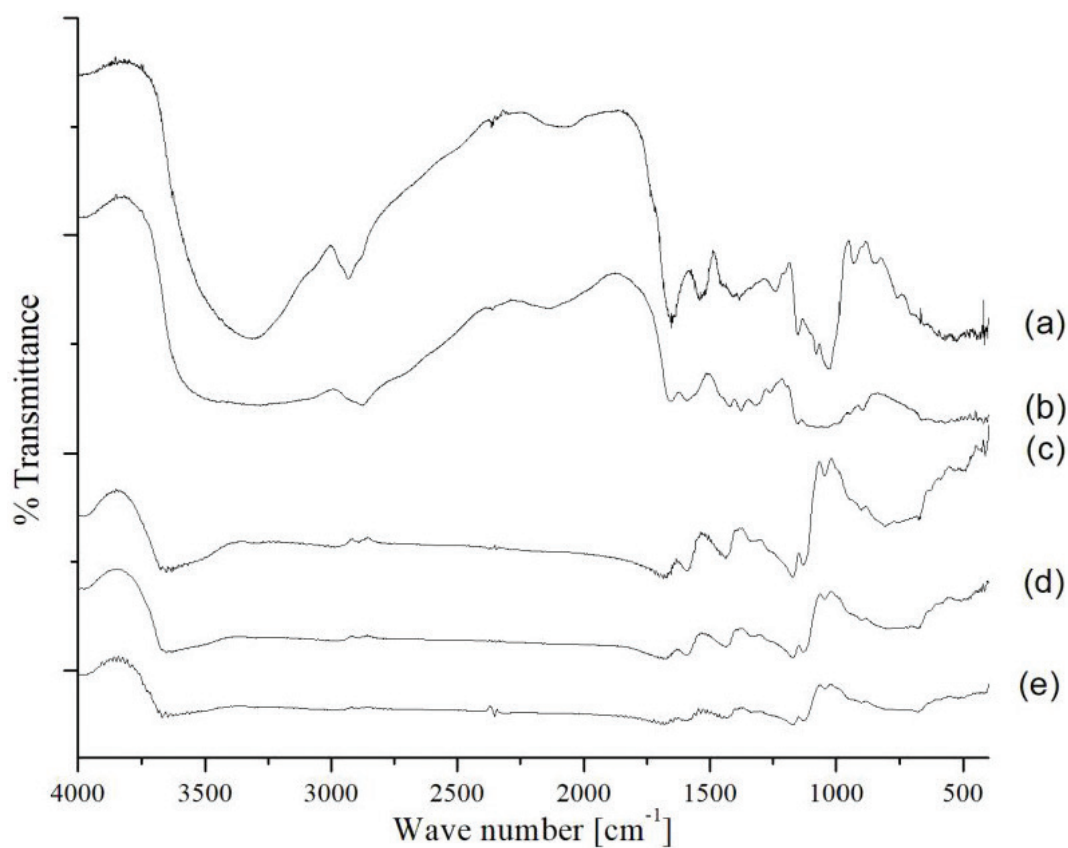


**Figure 4.** FTIR spectra of (a) bromelain, (b) powder chitosan, (c) CF, (d) CGF, and (e) bromelain encapsulated in CGF.

**Table 4.** Degrees of crosslinking and swelling ratios of hydrogels ( $n = 3$ ).

Hydrogel	Average of the degree of crosslinking (%)	Average swelling ratio (%)
CF	$0.48 \pm 0.02$	$3078.84 \pm 105.31$
CGF	$84.37 \pm 0.09$	$76.60 \pm 1.15$

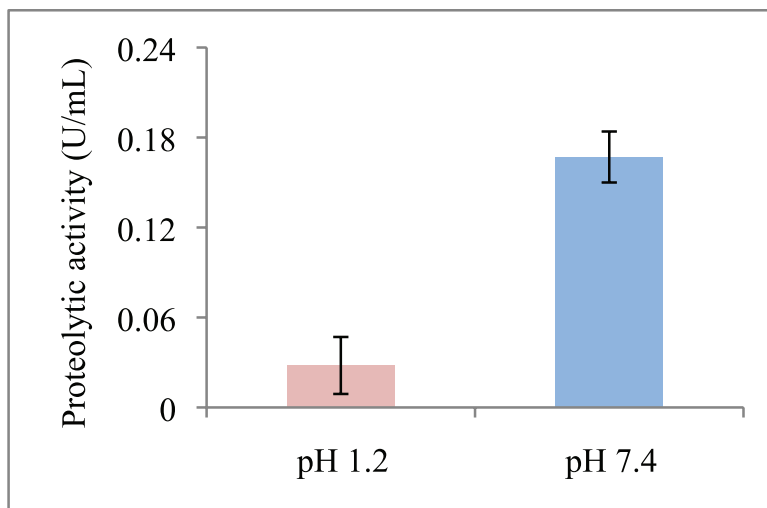
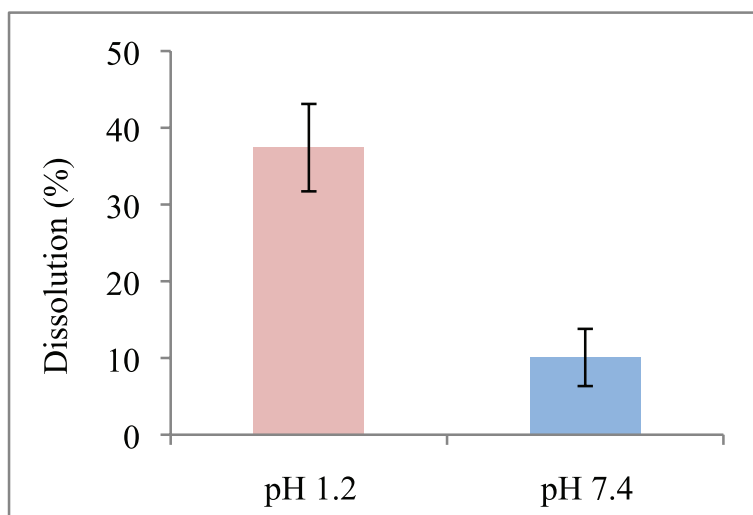
after encapsulation (Fig. 3). In particular, the encapsulation of bromelain produced bubbles on hydrogels and led to smaller and rougher surfaces. In the subsequent FTIR analyses of hydrogels, a similar band was observed before and after encapsulation (Fig. 4d and e), thus indicating that no new bonds were formed following the addition of bromelain and that bromelain was absorbed well in CGF. The physical interactions between bromelain and CGF were due to hydrogen bond interactions, as indicated by changes in intensity at  $3,500\text{--}3,080\text{ cm}^{-1}$  (Ataide *et al.*, 2017). Furthermore, the absorption band shifted from  $1,685$  to  $1,693\text{ cm}^{-1}$ .

**Table 5.** Efficiency of bromelain encapsulation into CGF ( $n = 3$ ).

Material	Protein levels loaded ( $\mu\text{g/ml}$ )	Proteolytic activity loaded (U/ml)	Average of encapsulation efficiency (%)
CGF	$89.40 \pm 1.92$	$8.32 \pm 0.14$	$96.29 \pm 2.07$

### *In vitro* dissolution tests

Dissolution profiles were generated to determine the degree to which proteins or enzymes diffused out of the CGF matrix. Figure 5 shows that the proteolytic activity of bromelain in the artificial intestinal environment ( $0.17 \pm 0.02\text{ U/ml}$ ) was greater than that in artificial stomach fluids ( $0.03 \pm 0.02\text{ U/ml}$ ; Fig. 5). Moreover, the dissolution of bromelain in artificial stomach fluid ( $37.41\% \pm 5.70\%$ ) was higher than in the artificial intestinal environment ( $10.07\% \pm 3.73\%$ ), as shown in Figure 6. These observations reflect the properties of CGF (Fig. 7a and b), which were more stable in the artificial intestinal environment than in artificial stomach fluid. Furthermore, *in vitro* dissolution

**Figure 5.** *In vitro* proteolytic profile of bromelain encapsulated in CGF ( $n = 3$ ).**Figure 6.** *In vitro* dissolution profile of bromelain encapsulated in CGF ( $n = 3$ ).

tests (Fig. 7c) caused the erosion of the hydrogel surface, and the resulting holes in CGF appeared during the first 2 hours immersion in acidic solutions (pH 1.2) and became larger when CGF was immersed in a pH 7.4 solution for 10 hours. The constant influx of artificial stomach fluid and intestinal solutions through the matrix forced bromelain out of the CGF through the holes. The scanning electron microscopy (SEM) micrographs of the surfaces and cross-sections of amorphous CGF after encapsulation and dissolution tests (Fig. 8) show the cross sections of CGF and confirm that bromelain successfully entered CGF. Specifically, the image in Figure 8a shows bromelain in the middle of the CGF matrix, and the morphological micrograph in Figure 8b indicates an even spread of bromelain on the CGF surface. Subsequent dissolution tests

caused bromelain to diffuse and escape the CGF, as indicated by the heterogeneous white spot of bromelain and the dark background of CGF (Fig. 8c and d).

## CONCLUSION

In this study, we isolated bromelain from pineapple cores and purified the enzyme by using ammonium sulfate fractionation and anion exchange chromatography with DEAE-cellulose resin. The highest specific activity (purest enzyme fraction) of bromelain was obtained from anion exchange chromatography. We also showed that CGF maintains bromelain activity until it is exposed to intestinal environments. Finally, the proteolytic activity of bromelain was greater in the artificial intestinal environment than in the artificial stomach fluid.

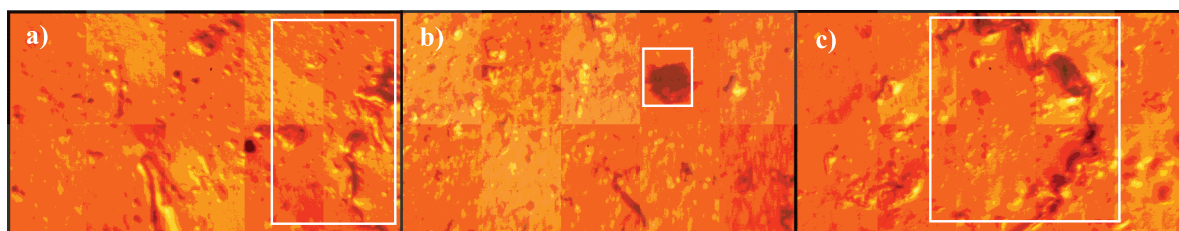


**Figure 7.** Morphological structure analyses of CGF matrix dissolution using an optical microscope at 45 $\times$  magnification; (a) CGF in solution at pH 1.2 for 2 hours, (b) CGF in solution at pH 7.4 for 10 hours, and (c) CGF after *in vitro* tests; pH 1.2 for 2 hours followed by pH 7.4 for 10 hours.

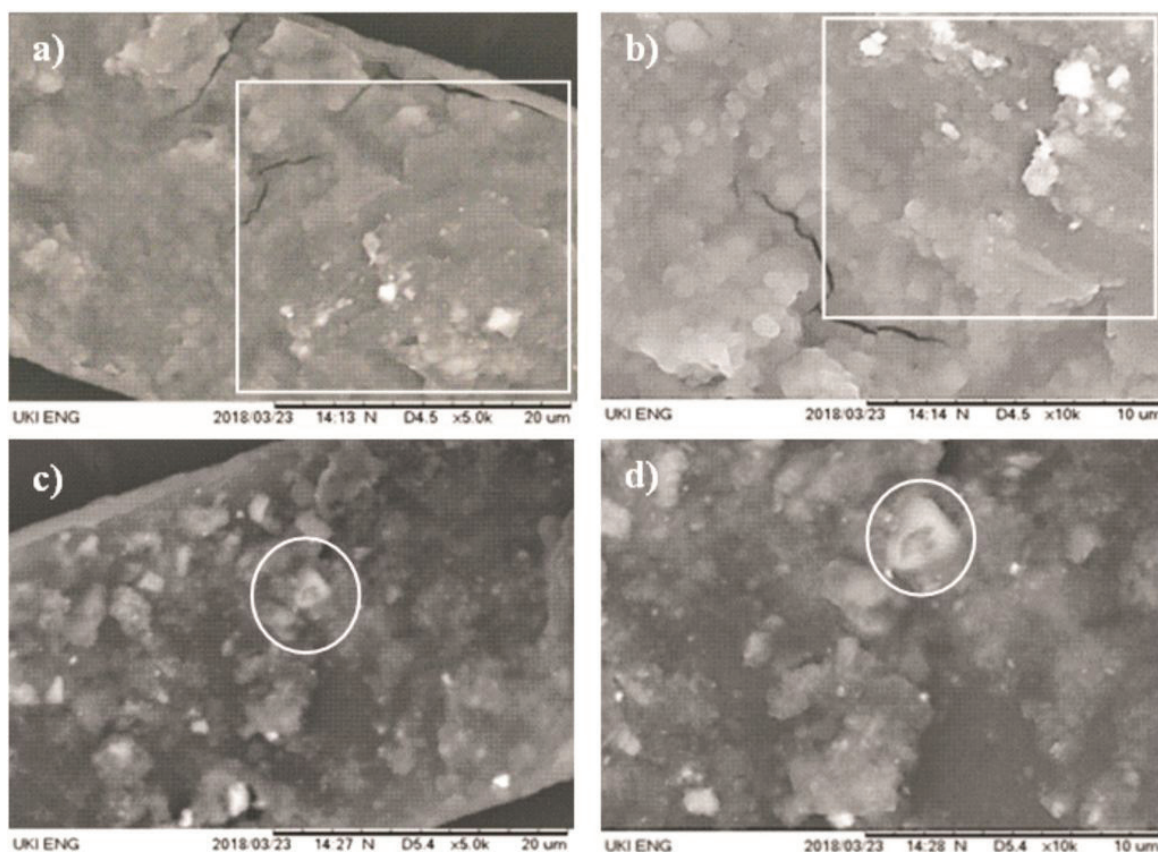


**Figure 8.** SEM micrographs of CGF matrixes after encapsulation; (a) cross section, 5,000 $\times$  magnification; (b) surface, 10,000 $\times$  magnification; CGF matrixes after dissolution test; (c) cross section at 5,000 $\times$  magnification; (d) surface at 10,000 $\times$  magnification.

## FUNDING

This research was financially supported by the Penelitian Dasar Unggulan Perguruan Tinggi (PDUPT) 2018 program of the Ministry of Research, Technology and Higher Education of the Republic of Indonesia.

## REFERENCES

- Ataide JA, Cefali LC, Rebelo MdA, Spir LV, Tambourgi EB, Jozala AF, *et al.* Bromelain loading and release from hydrogel formulated using alginate and arabic gum. *Planta Med*, 2017; 83:870–6.
- Abdel-Mohzen AM, Aly AS, Hrdina R, Montaser AS, Hebeish A. Eco-synthesis of PVA/chitosan hydrogels for biomedical application. *J Polym Environ*, 2011; 19:1005–12.
- Banerjee S, Siddiqui L, Bhattacharya S, Kaity S, Ghosh A, Chattopadhyay P, *et al.* Interpenetrating polymer network (IPN) hydrogel microspheres for oral controlled release application. *Int J Biol Macromol*, 2010; 50:198–206.
- Bernela M, Ahuja M, Thakur R. Enhancement of anti-inflammatory activity of bromelain by its encapsulation in katira gum nanoparticles. *Carbohydr Polym*, 2016; 143:18–24.
- Budianto E, Muthoharoh SP, Nizardo NM. Effect of crosslinking agents, pH and temperature on swelling behavior of cross-linked chitosan hydrogel. *Asian J App Sci*, 2015; 3:581–8.
- Chobotova K, Vernallis AB, Majid FAA. Bromelain's activity and potential as an anti-cancer agent: current evidence and perspectives. *Cancer Lett*, 2010; 290:148–56.
- Costa HB, Fernandes PMB, Romão W, Ventura JA. A new procedure based on column chromatography to purify bromelain by ion exchange plus gel filtration chromatographies. *Ind Crops Prod*, 2014; 59:163–8.
- Croisfelt F, Martins BC, Rescolino R, Coelho DF, Zanchetta B, Mazzola PG, *et al.* Poly(N-Isopropylacrylamide)-co-acrylamide hydrogels for the controlled release of bromelain from agroindustrial residues of ananas comosus. *Planta Med*, 2015; 81:1719–26.
- Devakate RV, Patil VV, Waje SS, Thorat BN. Purification and drying of bromelain. *Sep Purif Technol*, 2009; 64:259–64.
- Gautam SS, Mishra SK, Dash V, Goyal AK, Rath G. Comparative study of extraction, purification and estimation of bromelain from stem and fruit of pineapple plant. *Thai J Pharma Sci*, 2010; 34:67–76.
- Gonçalves VL, Laranjeira MCM, Fávere VT. Effect of crosslinking agents on chitosan microspheres in controlled release of diclofenac sodium. *Polímeros Ciência Tecnologia*, 2005; 15:6–12.
- Green AA, Hugesh WL. Protein solubility on the basis of solubility in aqueous solutions of salt and organic solvents. *Methods Enzymol*, 1955; 1:67–90.
- Ketnawa S, Chaiwut P, Rawdkuen S. Pineapple wastes: a potential source for bromelain extraction. *Food Bioprod Proc*, 2012; 90:385–91.
- Morris G, Castile J, Smith A, Adams GG, Harding SE. Macromolecular conformation of chitosan in dilute solution: a new global hydrodynamic approach. *Carbohydr Polym*, 2009; 76:616–21.
- Musfiroh FF, Setiasih S, Handayani S, Hudiyo S, Ilyas NM. In vivo antiplatelet activity aggregation assay of bromelain fractionate by ethanol from extract pineapple core (*Ananas comosus* [L.] Merr). *IOP Conf Ser Mat Sci Eng*, 2018; 299:1–4.
- Ou A, Bo I. Chitosan hydrogels and their glutaraldehyde-crosslinked counterparts as potential drug release and tissue engineering system-synthesis, characterization, swelling kinetics and mechanism. *J Phys Chem Biophys*, 2017; 3:1–7.
- Reddy GV, Reddy NS, Nagaraja K, Rao KSVK. Synthesis of pH responsive hydrogel matrices from guar gum and poly (acrylamide-co-acrylamidoglycolic acid) for anti-cancer drug delivery. *J App Pharm Sci*, 2018; 8:84–91.
- Respati E. Outlook nenas. Pusat Data dan Sistem Informasi Pertanian Sekretariat Jenderal Kementerian Pertanian, Jakarta, Indonesia, 2016.
- Selvakumaran S, Muhamad II, Razak SI. Evaluation of kappa carrageenan as potential carrier for floating drug delivery system: effect of pore forming agents. *Carbohydr Polym*, 2016; 135:207–14.
- Setiasih S, Darwis AAC, Dzikria V, Hudiyo S. Stability test of partially purified bromelain from pineapple (*Ananas comosus* (L.) Merr) core extract in artificial stomach fluid. *IOP Conf Ser Mater Sci Eng*, 2018; 299:1–7.
- Waterborg JH. The lowry method for protein quantitation. In: Walker JM (ed.). *The protein protocols handbook second edition*. Humana Press, New Jersey, pp 7–9, 2002.
- Yadav HKS, Shivakumar HG. In vitro and in vivo evaluation of pH-sensitive hydrogel of carboxymethyl chitosan for intestinal delivery of theophylline. *ISRN Pharm*, 2012; 2012(article ID 763127):1–9.
- Zhao HR, Wang K, Zhao Y, Pan LQ. Novel sustained-release implant of herb extract using chitosan. *Biomaterials*, 2002; 23:4459–62.

### How to cite this article:

Setiasih S, Prabowo HA, Budianto E, Hudiyo S. Dissolution profiles of partially purified bromelain from pineapple cores [*Ananas comosus* (L.) Merr] encapsulated in glutaraldehyde-crosslinked chitosan. *J App Pharm Sci*, 2018; 8(10): 017-024.